- B. Bechtle
- C. Schünemann
- G. Skudelny
- V. Zimmermann

# **Delayed Closed-Loop Scheme for Stepping Motor Control**

Abstract: An efficient method for control of stepping motor speed and position, the delayed closed-loop (DCL) mode, is described. The new technique permits control of high-speed motor motion by means of a programmed speed-displacement characteristic. The method combines the static-speed control characteristic of the open-loop mode with the stable dynamic behavior of the closed-loop mode. Unlike other schemes for delayed closed-loop control, the present configuration features an extension of delay time to more than one step duration, significantly improving the velocity control. The phase angle can also be varied to  $\pm 180^{\circ}$ , permitting adequate control of deceleration as well as acceleration. A stability analysis is made of the DCL control method. In an illustrative example, the technique is applied to control of the carriage drive on an experimental high-speed line printer.

#### Introduction

Electrical stepping motors [1, 2] can be operated in the start-stop mode for low-speed position control and in the slewing mode for higher speed applications. In the start-stop mode the motor is actuated by an electrical pulse representing a step and then reaches the new position and comes to a stop before the next pulse is applied.

This paper describes a slewing-mode control method for precise high-speed positioning with a large number of steps, as required for a paper carriage drive in fast line printers. The motor accelerates for a certain number of steps, subsequently moves for several steps at constant high speed, and decelerates to a stop in a third sequence of steps. The objective is to achieve the fastest possible carriage drive in combination with precise position control according to the programmed number of steps.

The two conventional control techniques [3], the open-loop mode and the closed-loop mode, are first reviewed and some problems are discussed, leading to the development objective of a high-speed slewing operation

The open-loop mode is an enforced speed control method. The motor simply follows the programmed sequence of steps. This mode is adequate for low-speed operation, e.g., the start-stop mode. With a continuously applied sequence of steps in the high-speed slewing mode, however, the motor tends to oscillate. This occurs because the step sequence must be programmed so that the motor can follow with worst-case parameter tolerances and load conditions. With relaxed load conditions, the motor torque exceeds the required value. The motor

responds by correcting its phase angle in electrical and mechanical oscillations. The motor may then fall out of synchronization.

The closed-loop mode represents a strong feedback of the motor phase angle  $\delta$ . Any motor-advance pulse, or step, is started by a feedback pulse generated by means of a timing disk indicating the position achieved. The phase angle is thus stabilized and oscillations do not occur.

The motor torque is a function of the phase angle  $\delta$  between the driving voltage and the internally generated emf. The optimum phase angle as a function of motor speed increases from practically zero at low speeds to  $90^{\circ}$  at high speeds. In the closed-loop mode, this phase angle corresponds to the electrical angle between the motor-advance (MA) pulse and the feedback (FB) pulse, as indicated in Fig. 1. Usually, the timing disk is firmly attached to the rotor and adjusted so that the angle is approximately zero. When an additional pulse is injected, it is switched abruptly to  $90^{\circ}$  [3, 4]. With certain delay techniques, the phase angle can also be varied continuously [3, 4]. The range of variation is smaller than  $90^{\circ}$  with these techniques, which is insufficient for full acceleration and deceleration.

The problem of the closed-loop control mode is that the motor speed is unregulated and strongly dependent on load conditions and motor parameter tolerances. The motor accelerates or decelerates according to the driving torque and load conditions. Thus, the motor speed after a programmed number of steps is not defined and pre-

235

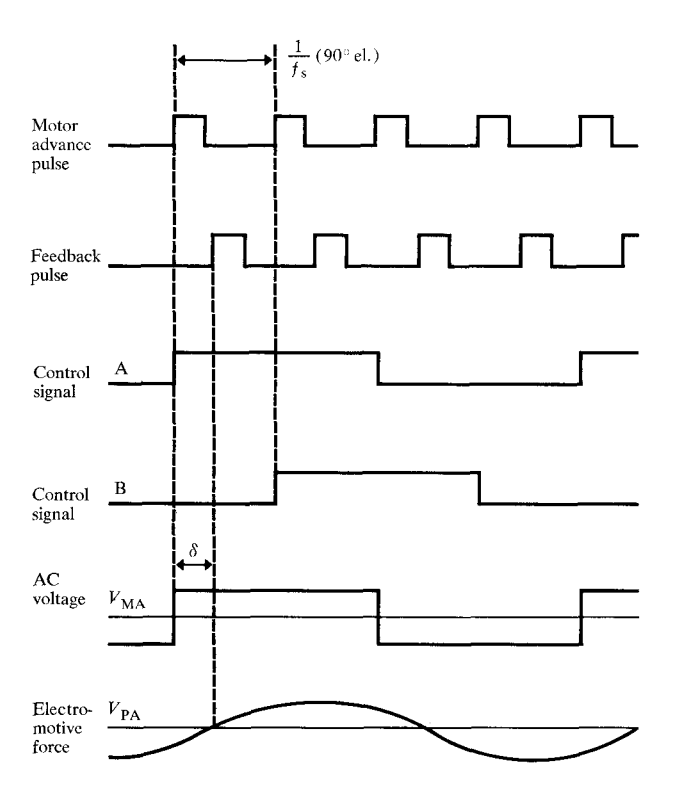


Figure 1 Control signals and voltages for a two-phase motor.

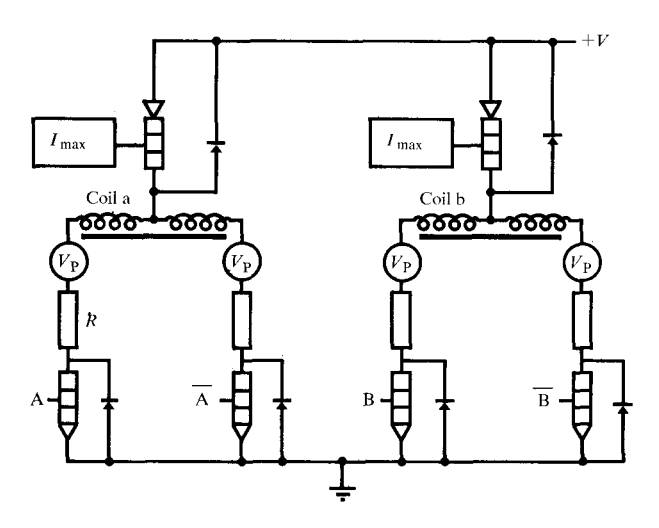


Figure 2 DC/AC converter-type circuit used in sequencing the motor drive signals.

cise stop control is not feasible. After the programmed number of steps, the motor may still have a positive or negative velocity. The usual way to solve this problem is to terminate the deceleration phase when a certain well-controllable, low-speed level is achieved. The motor is run at this low speed for all but the last three or four programmed steps and finally stops with these three or four steps in the open-loop mode. The length of the low-

speed phase compensates for different motions in the high-speed phase. However, the low-speed phase also increases the overall positioning time significantly. For both reasons, the closed-loop mode seems inadequate for high-speed, large-motion applications.

The control method discussed in this paper is the delayed closed-loop (DCL) mode, which allows motor motion with the shortest possible slewing time, without losing stability and with accurate positioning. The DCL mode exploits the time-delayed closed-loop schemes [4] in a more general way, offering better tradeoffs between stability and performance and allowing optimally tuned design. Unlike the known delayed closed-loop schemes, the DCL mode delay is extended to several step durations, providing good speed control and a wider phase angle, e.g., to ±180°. An external velocity-control system to vary the time delays [5] is thus avoided. Control is based on a programmed delay step number table. Because of the inherent velocity control, the motor effectively follows a fictive speed-time characteristic. This method was proved and applied to a high-speed printer paper carriage drive. The experimental setup was run under control of a small computer having the timedelay table stored in a memory.

Several sequencing circuitries are in use [6] which, from a performance point of view, differ in power efficiency. For this work, a simple dc/ac converter circuit (shown in Fig. 2) with voltage clamp and current threshold control has been chosen.

In the following section, the basic sequencing logic is described and the average motor torque calculated as a function of phase angle and stepping frequency. This torque function is the input to a computer simulation of system motion. The simulation yields a suitable delayinterval table for the actual DCL control. A description of the basic DCL operation is given in the third section, and this control mode is analyzed for stability in the subsequent section. The analytical results give the limiting conditions for the motion simulation and delayinterval table, restricting the motor torque to a point somewhat below its maximum value. In the last section, experimental measurements are presented.

# Motor characteristics and operation

# Physical description

The stepping motor utilizes a two-phase, permanent magnet rotor. The stator has two coils that are displaced by 90° physically and electrically and are driven by two separate drivers, as shown in Fig. 2. Each coil consists of two half-coils with center taps which are bifilar-wound and operated one at a time. The two drivers are controlled by signals A and B and generate two ac voltages  $V_{\rm MA}$  and  $V_{\rm MB}$ , which are displaced electrically by

90° (Fig. 1). Signals A and B are triggered by the motor advance (MA) pulses with the stepping frequency  $f_s$  and switched cyclically  $(\overline{AB}, AB, \overline{AB}, \overline{AB}, \overline{AB}, \cdots)$ . At the commutation from A to  $\overline{A}$ , the coil current is transferred to the other half-coil in the backward direction. The driving voltage then commutates current and magnetic field into the new positive direction. The commutation time is determined by the driving voltage  $V_M$ , the half-coil inductance L, and the half-coil resistance R. With increasing motor speed, an additional voltage has to be taken into account, the emf  $V_P$ . The rotor magnet generates this voltage in the stator coils. There are two voltages,  $V_{PA}$  and  $V_{PB}$ , electrically displaced by 90°, corresponding to the two stator coils. The electrical angle between  $V_M$  and  $V_P$  is  $\delta$ .

The coil current is limited to a maximum  $I_{\text{max}}$  for motor protection. Current threshold is provided by a servo-controlled chopper device, instead of the usual resistor network.

Switching of the stepping signal from A to  $\overline{A}$  and the accompanying zero-transition of the voltage  $V_{MA}$  are started by a motor advance (MA) pulse (Fig. 1). The timing disk for feedback (FB) pulse generation normally is adjusted so that the FB pulse is generated with a zero transition of the emf  $V_{PA}$ . The phase angle  $\delta$  then corresponds electrically to the time interval between MA and FB.

In the next section the average motor torque in the slewing mode is calculated for a given threshold current, as a function of stepping frequency and phase angle.

## • Motor torque

The motor runs with a mechanical angular velocity

$$\Omega = \omega/N = 2\pi f_s/4N = \pi f_s/2N, \tag{1}$$

where  $\omega$  is the electrical angular frequency (e.g., of  $V_{\rm P}$  and  $V_{\rm M}$ ), N is the number of rotor teeth, and  $f_{\rm s}$  is the stepping frequency. Thus, one step corresponds electrically to 90°.

The emf  $V_P$  is considered to be sinusoidal and proportional to the mechanical velocity, where

$$V_{\rm p} = K \Omega \sin (\omega t - \delta), \tag{2}$$

t=0 being related to the zero transition of  $V_{\rm M}$ .

The constant K can be measured using (2) when the motor is operated as generator without load.

The mechanical motor power is

$$P_{\rm mech} = T \,\Omega,\tag{3}$$

in which T is the motor torque.

Motor losses are neglected and the mechanical power is then equal to the electrical power:

$$P_{el} = 2V_P(t) I(t) = T(t) \Omega, \tag{4}$$

I(t) being the coil current, which flows alternately in each half-coil. Combining (2) and (4) we obtain

$$T(\omega, \delta, t) = 2KI(\omega, \delta, t) \sin(\omega t - \delta). \tag{5}$$

The average torque, from integration over a half-period, is

$$T_{\rm av}(\omega, \delta) = 2K\omega/\pi \int_0^{\pi/\omega} I(\omega, \delta, t) \sin(\omega t - \delta) dt. \quad (6)$$

To solve Eq. (6), the function  $I = I(\omega, \delta, t)$  must be calculated. The differential equation for the current I(t) is

$$L(dI/dt) + RI = V_{M} - V_{D}, \tag{7}$$

where L is the half-coil inductance and R is the half-coil resistance.

The solution of the homogeneous part of (7) is

$$I + Ce^{-(R/L)t}. (8)$$

Calculating the inhomogeneous equation by using the method of variation of the constant, we find

$$I = C(t) e^{-(R/L)t}, (9)$$

$$dI/dt = dC/dt \ e^{-(R/L)t} - C(t) (R/L) e^{-(R/L)t}. \tag{9a}$$

Inserting into (7) and using (9) we obtain

$$dC/dt = (V_{\rm M} - V_{\rm P})(1/L)e^{(R/L)t}$$
(10)

With (2), C(t) becomes

$$C(t) = \int_0^t \frac{V_M}{L} e^{\frac{R}{L}t'} dt' - \frac{K\omega}{NL} \cdot \int_0^t e^{\frac{R}{L}t'} \times \sin(\omega t' - \delta) dt'.$$
(11)

Equation (11) is solved

$$C(t) = \frac{V_{M}}{R} \left( e^{+\frac{R}{L}t} - 1 \right) - \frac{K\omega}{NL\left(\frac{R^{2}}{L^{2}} + \omega^{2}\right)}$$

$$\times \left\{ e^{+\frac{R}{L}t} \left[ \frac{R}{L} \sin(\omega t - \delta) - \omega \cos(\omega t - \delta) \right] + \left[ \frac{R}{L} \cdot \sin\delta + \omega \cdot \cos\delta \right] \right\} + I_{0}$$

and inserted into (9).

$$I(t) = \frac{V_{\rm M}}{R} \left(1 - e^{-\frac{R}{L}t}\right) - \frac{K\omega}{NL\left(\frac{R^2}{L^2} + \omega^2\right)}$$

$$\times \left[\frac{R}{L}\sin(\omega t - \delta) - \omega\cos(\omega t - \delta) + e^{-\frac{R}{L}t}\left(\frac{R}{L}\sin\delta + \omega\cos\delta\right)\right] + I_0 e^{-\frac{R}{L}t}. \tag{12}$$

237

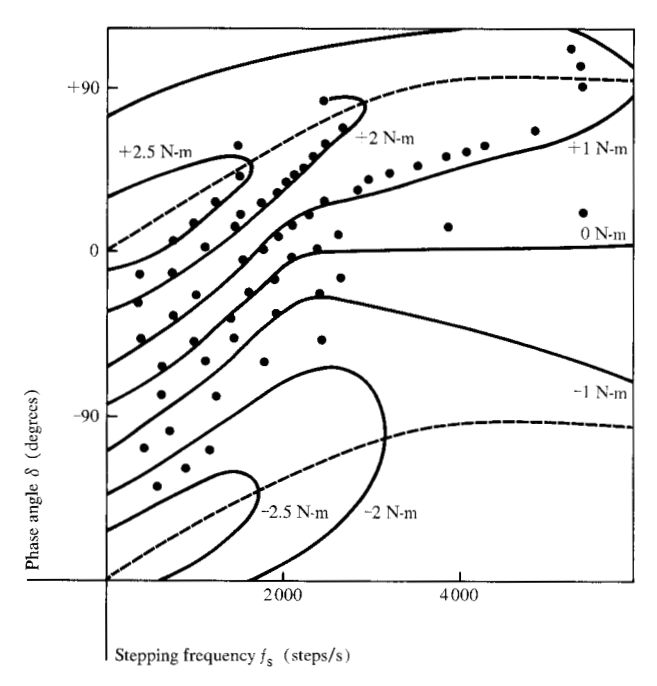


Figure 3 Computations (solid lines) and measurements (points) for the isotorque field, showing contour lines of equal torque as a function of stepping frequency and phase angle. The dashed lines represent maximum torque.

Figure 4 Principal pulse scheme and velocity control method for the delayed closed-loop mode, showing several DCL classes.

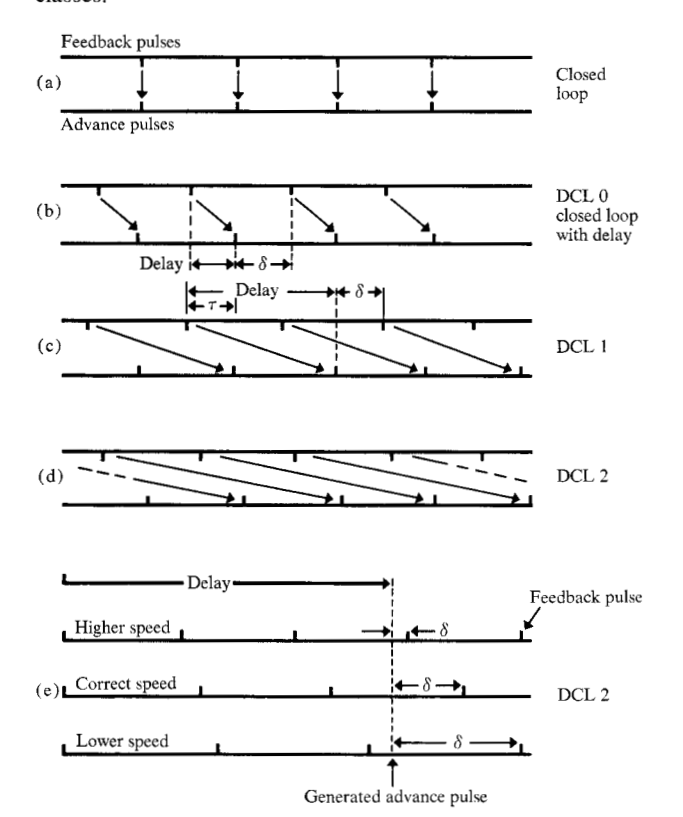


Table 1 Input parameters for the measurements of the isotorque field and for the stability analysis.

$$L = 0.0024 H$$

$$R = 0.7 \Omega$$

$$N = 36$$

$$K = 0.324 \text{ V-s}$$

$$V_p = 55 \text{ V}$$

$$I_{\text{max}} = 6.7 \text{ A}$$

$$J = 2 \times 10^{-4} \text{ kg-m}^2 \text{ (inertia of motor and load)}$$

The initial current  $I_0$  is calculated from the periodic boundary condition

$$I_{0} = I_{t=0} = -I_{t=\pi/\omega}$$

$$I_{0} = \frac{V_{M}}{R} \frac{1 - e^{-\frac{R\pi}{\omega L}}}{1 + e^{-\frac{R\pi}{\omega L}}} + \frac{K\omega(\frac{R}{L}\sin\delta + \omega\cos\delta)}{NL(\frac{R^{2}}{I^{2}} + \omega^{2})}$$
(13)

(12) and (13) combined yields

 $T(\omega, \delta) =$ 

$$I(t) = \frac{V_{\rm M}}{R} \left[ 1 - \frac{2e^{-\frac{R}{L}t}}{1 + e^{\frac{R\pi}{\omega L}}} \right] - \frac{K\omega}{NL\left(\frac{R^2}{L^2} + \omega^2\right)}$$

$$\times \left[ \frac{R}{L} \sin(\omega t - \delta) - \omega \cos(\omega t - \delta) \right]. \tag{14}$$

Inserting (14) into (5) and after solution of the integrals, we finally obtain

$$2K\frac{\omega}{\pi} \left[ \frac{2V_{\rm M}}{R\omega} \cos \delta - \frac{2V_{\rm M} \left( -\frac{R}{L} \cdot \sin \delta + \omega \cos \delta \right)}{R \left( \frac{R^2}{L^2} + \omega^2 \right)} - \frac{KR\pi}{2NL^2 \left( \frac{R^2}{L^2} + \omega^2 \right)} \right]$$
(15)

This solution is equivalent to that obtained in [7] by another method of calculation. However, the analytical form of  $T(\omega, \delta)$  is valid only for a special case of linearity, when the motor speed is high and the motor current is always smaller than the threshold determined by the chopping device. In general, the current I is limited to the threshold value  $I_{\text{max}}$ . In the calculation, this threshold behavior is now reflected by setting  $I = I_{\text{max}}$  if the current tends to exceed  $I_{\text{max}}$ . Under certain conditions it is possible that the emf decreases the current before the end of the half-period and causes a reentry into the nonchopped state.

(15)

The solutions of the differential equation (7) are still valid; however, the calculation of the time at which the current reenters the nonlimited state results in a transcendental equation.

To solve this transcendental equation, a numerical method is applied. The initial current value at t = 0 is determined iteratively. The function I(t) calculated in this way is inserted into (6) and the torque function of phase angle  $\delta$  and frequency  $\omega$  is integrated numerically.

The motor used in the experimental setup is a Superior Electric, type M93. The experimental parameters are given in Table 1.

Results of the computation are plotted in Fig. 3 in the form of an "isotorque" field showing contour lines of equal torque vs  $f_s$  and  $\delta$ . The maximum torque for a given stepping frequency is found at the point where the corresponding isotorque line has a vertical tangent. The dotted line connects these points and represents the optimum  $\delta(f_s)$  for maximum torque.

A part of the isotorque field was measured in the experimental setup and is represented by the points in Fig. 3. Agreement with the calculated figures is fair, considering that the measured torque is smaller because of internal motor friction and other losses. The isotorque field is the basic input parameter for the dynamic simulation and generation of the delay time table used for the experiments described in the section entitled "Implementation and experimental results."

## Delayed closed-loop (DCL) mode

In the DCL control scheme, the motor-advance pulse is generated from the feedback pulse with a certain delay. In contrast to conventional closed-loop mode and other time delaying techniques [4], the delay interval has a typical duration of more than one or two steps. Depending on the duration of the delay intervals, a number of DCL classes can be defined according to the scheme shown in Fig. 4.

Whereas in the conventional closed-loop mode [Fig. 4(a)], the motor advance pulse is immediately triggered by the feedback pulse, the first DCL class (called DCL 0), Fig. 4(b), provides a delay time  $t_d$  between the FB and the MA pulses, which corresponds electrically to an angle  $90^{\circ} - \delta$ .

In a second DCL class (DCL 1), Fig. 4(c), the delay time corresponds to an electrical angle  $180^{\circ} - \delta$  This class is even more effective with respect to speed control. The delay interval is larger than the duration of one step. This overlapping degree is called m = 1.

The delay intervals are controlled by counters, which in turn are triggered by the FB pulses. It can be seen that in the intervals  $\tau$  in Fig. 4 an overlapped action of two time counters is required in class DCL 1.

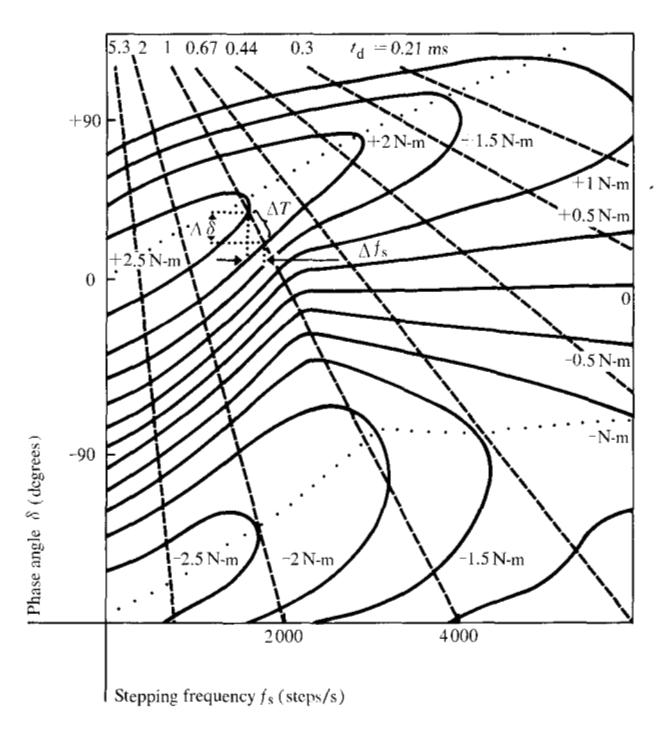
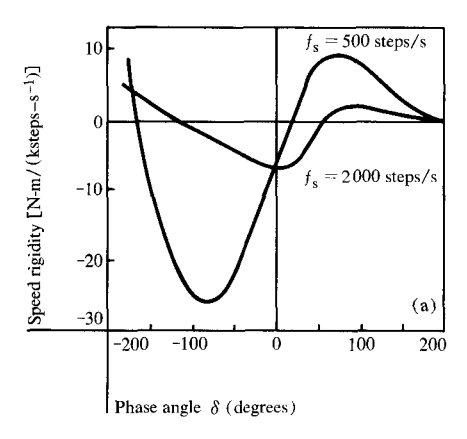


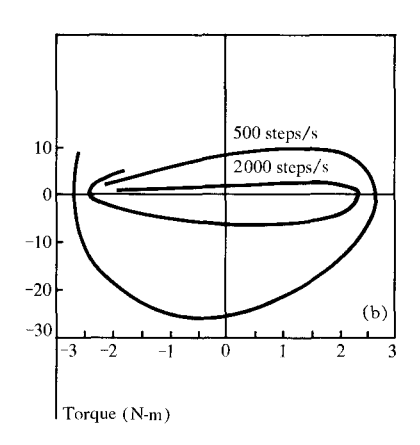
Figure 5 Relationships between frequency, torque, phase angle, and programmed delay times for given loads. The isotorque fields are indicated by solid curves and the phase angle by dashed lines. The degree of overlap is m = 1.

In a third class, DCL 2, the delay interval exceeds two step durations, as shown in Fig. 4(d). Three time counters are required at intervals  $\tau$ . The overlapping degree is m=2. The straightforward extension to an infinite overlapping degree (DCL  $\infty$ ) leads to the conventional open-loop mode.

In contrast to the conventional closed-loop system, the DCL mode stabilizes the motor speed by its inherent negative feedback, as indicated in Fig. 4(e).

During the delay time  $t_d$ , the motor proceeds at the correct speed and a certain angle until the corresponding MA pulse is generated. The phase angle  $\delta$  just corresponds to the required motor torque. With higher motor speed, the motor has turned with a larger displacement during the delay interval, thus reducing the phase angle  $\delta$ ; in the case of lower speed, the phase angle  $\delta$  is increased. Since an increased phase angle increases the motor torque and a decreased phase angle decreases the torque, the feedback mechanism acts to maintain the correct speed. With higher speed the torque is reduced and the motor decelerates, and vice versa. This mechanism works also for variable delay intervals-the motor follows the pulse sequence determined by the programmed delay times over the whole slewing range, including acceleration and deceleration phases.





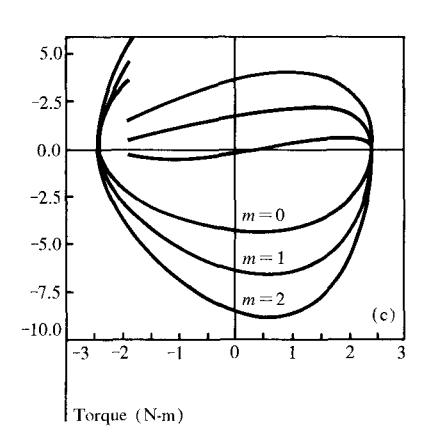


Figure 6 Analysis of speed stability under varying load: speed stability vs (a) phase angle for degree of overlap m=1; (b) torque, for m=1; and (c) torque for various degrees of overlap with  $f_s = 2000$  steps/s.

The DCL mode can be considered a transition from the closed-loop mode to the open-loop mode. It has a displacement feedback like the closed-loop mode and a speed stabilizing characteristic like the open-loop mode. By varying the degree m of overlapping, the design point can be shifted in either direction. On the other hand, the tendency of the system to oscillate grows with increasing m.

#### Stability analysis

A numerical analysis is made here of motor speed stability under varying load and dynamic behavior in the DCL mode. The input parameters are listed in Table 1.

• Analysis of speed stability under varying load

The motor torque is a function of the phase angle and angular frequency, according to Eq. (6). In the DCL mode the phase angle is related to the stepping frequency by

$$\delta = (\pi/2)(1+m) - (\pi/2)f_s t_d. \tag{16}$$

For small variations around a given operating point  $(f_{\rm s0},\,\delta_{\rm 0})$ , a linear approximation for the torque calculation is

$$\Delta T = \left(\frac{\partial T}{\partial f_{\rm s}}\Big|_{f_{\rm SO}, \ \delta_0} \times \Delta f_{\rm s}\right) + \left(\frac{\partial T}{\partial \delta}\Big|_{f_{\rm SO}, \ \delta_0} \times \Delta \delta\right). \tag{17}$$

Combining (16) and (17) we obtain

$$\frac{\Delta T}{\Delta f_{\rm s}} = \frac{\partial T}{\partial f_{\rm s}} \Big|_{f_{\rm s0}, \ \delta_0} - t_{\rm d} \frac{\pi}{2} \frac{\partial T}{\partial \delta} \Big|_{f_{\rm s0}, \ \delta_0}. \tag{18}$$

Figure 5 shows graphically how the phase angle is related to frequency for given loads. The diagram combines the isotorque field, Fig. 3, and the graphic representation of (16), for m = 1. The nominal load is

assumed to be 2N-m and the programmed delay time  $t_{\rm d}=1$  ms. The intersection of the 2N-m-torque curve with the delta( $f_{\rm s}$ )-line defines the operating point. A small load variation  $\Delta T$  results in deviations  $\Delta \delta$  and  $\Delta f_{\rm s}$ .

The ratio of  $\Delta T/\Delta f_{\rm s}$  is a measure of the speed stability of the operating point  $(f_{\rm so},\,\delta_{\rm o})$ . A large value of  $\Delta T/\Delta f_{\rm s}$  means that a large load variation is required to get some velocity deviation. Thus, high stability against load variations is desirable for a powerful speed control system.

The ratio  $\Delta T/\Delta f_{\rm s}$  is negative for stable operating points, i.e., lower velocity causes the motor to generate higher torque. Positive values of  $\Delta T/\Delta f_{\rm s}$  characterize an unstable condition.

The stable and unstable ranges are indicated by the point lines in Fig. 5. The area between the two lines corresponds to a stable condition. For positive torque, the maximum torque curve (Fig. 3) is just inside the stable area. For negative torque, this curve falls slightly into the unstable area. With the motor deceleration phase, therefore, the delay interval table must be programmed so that the torque is somewhat below its maximum.

In Figs. 6(a) and 6(b), speed rigidity is plotted versus phase angle and torque, respectively. The step frequency is held as a constant parameter. Figure 6(b) shows that with respect to torque and speed rigidity, there can be a conflicting situation: Large torque is associated with poor speed stability under varying load, and vice versa.

Only a small amount of the motor torque, however, need be sacrificed to obtain reasonable speed control. Speed stability and speed control are better with lower velocities, which is significant for accurate stopping control.

When the degree of overlap m is increased, the speed is more stable. Figure 6(c) shows speed stability vs

torque for a constant step frequency of 2000 step/s and various values of m. Besides the tendency of the system to oscillate with large m, the cost of the servomechanism increases. This must be traded with the required speed and position control accuracy.

Note that in Figs. 6(a) through 6(c) the positive speed stability curves characterize an unstable situation.

#### • Dynamic analysis

So far, stability and speed control as functions of load and design parameters have been analyzed for steady state operation. Now the transition between two load conditions is discussed. Using (17), a block diagram of the system for the Laplace-transformed variables can be drawn, Fig. 7. It is valid for small deviations from a steady state condition; the notations  $\delta_1$ ,  $T_1$ , etc., characterize the small-signal responses to the load variation  $\Delta T$ , and s is the Laplace operator. The outputs of blocks 1 and 2 add to the motor torque according to (17). The mechanical load is varied by  $\Delta T$ , resulting in a net torque which accelerates or decelerates the mechanical system. The output of integrator 3 is the angular frequency  $\omega_1 = (\pi/2) f_s$ . The block operator is  $K_3 =$ N/J, N being the number of rotor teeth and J the inertia. The output of integrator 4 is the displacement. According to (17), the angular frequency is the input to block 1.

In the DCL mode the MA pulse is generated by the FB pulse after a delay interval  $t_d$ . The generation of FB pulses corresponds to the displacement. Block 5 and the summing point represent the relation (16).

Figure 8 shows the speed response  $f_{\rm s1}/\Delta T = f(t)$  for a small load step with the various control schemes applied. The steady state of the speed response is the inverse speed stability. The response function was obtained by modifying the block diagram of Fig. 7 in the following ways:

#### 1. Delayed closed-loop control

The block diagram can be translated into

$$\left\{ -\Delta T + \omega_1 K_1 + \frac{\omega_1}{s} \left[ \exp(-st_d) - 1 \right] K_2 \right\} \frac{K_3}{s} = \omega_1. \quad (19)$$

With  $f_{s1} = (2/\pi)\omega_1$  explicitly:

$$f_{s1} = \frac{2}{\pi} \left\{ \frac{-K_3 s \Delta T}{s^2 - K_1 K_2 s + K_2 K_3 [1 - \exp(-st_d)]} \right\}.$$
 (20)

## 2. Closed-loop control

The phase angle  $\delta$  is constant; therefore the input to block 2 is zero. Equation (20) simplifies to

$$f_{\rm s1} = \frac{2}{\pi} \left[ \frac{-\Delta T}{\left( -K_1 + \frac{s}{K_1} \right)} \right]. \tag{21}$$

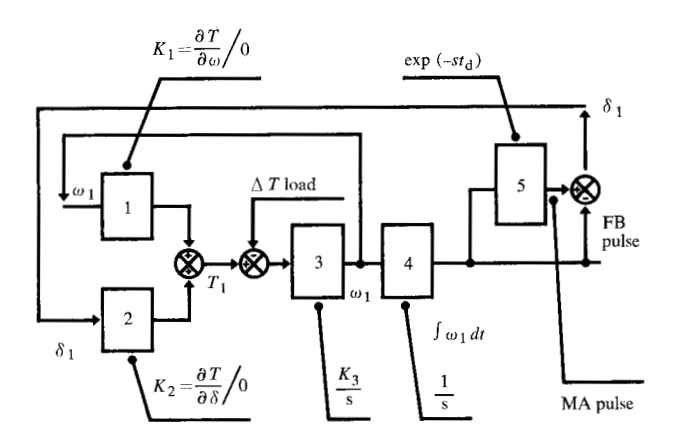


Figure 7 Block diagram for small-signal deviations.

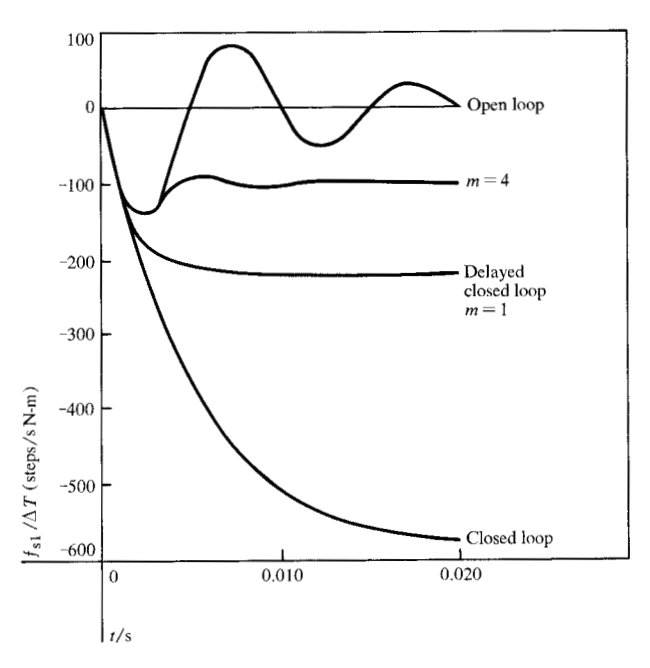


Figure 8 Load step response for various control schemes;  $\delta = 30^{\circ}$ ,  $f_s = 2000$  steps/s.

## 3. Open-loop control

The MA pulses are generated by an independently operating clock. Block 5 has no input and is omitted. Equation (20) simplifies to

$$f_{s1} = \frac{2}{\pi} \left( \frac{-sK_3\Delta T}{s^2 - sK_1K_3 + K_2K_3} \right). \tag{22}$$

Figure 8 again demonstrates the tradeoff property of DCL control. With increasing m, speed stability under load and speed control are improved, with the extreme case of open-loop mode. On the other hand, the ten-

241

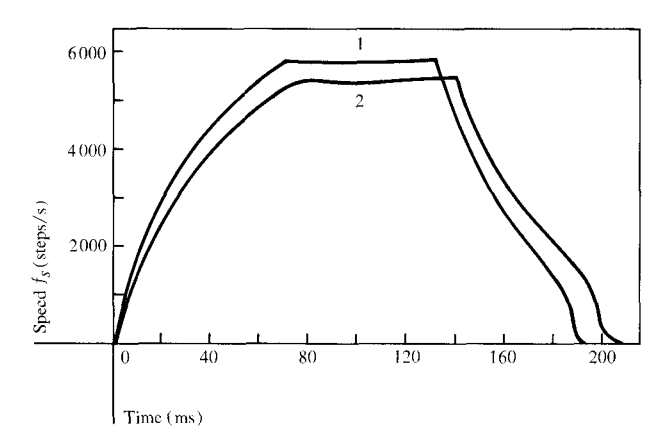


**Figure 9** Measurements of the velocity-vs-time line-printer carriage driven by a stepping motor: curve 1, without paper; curve 2: with six-part paper.

dency to oscillate is also increased, starting with m = 4. The design points m = 1 to 3 represent a good compromise between the two conflicting parameters.

## Implementation and experimental results

The DCL-controlled stepping motor was used experimentally to drive the paper carriage of a high-speed printer. The control was implemented by a hard-wired control computer having the delay-interval tables stored in a memory. Depending upon carriage conditions, motion length as well as inertia and friction varied over a wide range.

#### • Generation of the delay interval table

The delay interval-vs-step number table represents effectively the programmed motor speed curve. The actual speed curve deviates from the programmed one depending on the degree of overlapping, motor parameter tolerances, and load variations. The delay-interval table for the shortest possible positioning time was calculated, with the isotorque field and the motion simulation as inputs. The isotorque field relates delay times to stepping frequency, or velocity, along a defined torque-stepping frequency curve. The curve ideally would be the maximum torque curve but with respect to stability and adequate speed control, the torque is somewhat smaller. With the chosen function  $T(\Delta, f_s)$  the motor run simulation is performed, bringing the mechanical inertia into the calculation. The simulation outputs are the speedtime and speed-step characteristics. From the latter, in combination with the data in Fig. 5, the associated delay interval is derived for each step.

Note that this procedure is based on a steady state model, i.e., on the assumption that the motor torque is constant over the duration of one step. This assumption is sufficiently accurate for all but the first and last few steps. With these few steps the proper delay intervals for optimum torque were obtained experimentally.

#### • Implementation

The delay interval words stored in the memory are addressed by the step number. With the specific application to the carriage drive, a variety of different positioning lengths must be provided according to the different paper skips. To conserve storage capacity, the various runs are composed in modules by run elements: acceleration and deceleration phases and a constant-speed phase. Small runs consist of short acceleration and deceleration elements only. With larger runs, longer acceleration and deceleration phases are required. These are composed of the short deceleration and acceleration elements. Very long runs require an additional constant-speed phase. Thus, in addition to the delay interval table, the program for linking the different run elements must be stored in memory.

Delay-time control is implemented by counters. Triggered by the feedback pulse, the memory loads the  $t_{\rm d}$  value into the counter which starts counting downward; at zero, an MA pulse is generated. The larger the overlap degree m, the more counters must operate simultaneously.

#### • Experimental results

The delay-interval table consists of 170 steps for acceleration and 130 steps for deceleration. The speed-vs-time curves in Fig. 9 were measured without paper (curve 1, load friction 0.3 N-m) and with six-fold paper on the carriage (curve 2, load friction 0.45 N-m). The deviations in velocity and positioning time are small, thus demonstrating the control behavior of the system. Accurate stop control, i.e., full stop after the programmed step number, is provided in both cases.

The speed-time characteristic fully utilized the motor torque over the entire motion interval. In addition, because of the excellent velocity control with low speed, the actual speed-time curve was nearly identical for both load conditions. This is significant with paper drive, since now the paper tension is independent of load conditions.

Figure 10 shows measured states of the phase angle as a function of stepping frequency. This plot also demonstrates the speed control behavior. With acceleration, the time-interval table is calculated for maximum load friction of 0.45 N-m. With zero load friction, the system reduces the phase angle, and therefore the motor torque, automatically. With deceleration, the time interval table is calculated for zero friction load, i.e., maximum required motor torque. With full load friction, less motor torque is required and again the phase angle is reduced.

## **Summary**

A simple but efficient method for speed and position control of stepping motors, the delayed closed-loop mode, has been developed as described. The DCL mode provides high-speed slewing motion along a defined speed-displacement characteristic, including deceleration to a stop, under a wide range of load conditions. The method combines the static speed control characteristic of the open-loop mode with the stable dynamic behavior of the closed-loop mode. It also provides the flexibility of moving the design point toward the operating characteristics of either the open-loop or the closed-loop scheme.

The DCL mode runs under control of a programmed delay time-step number table stored in a memory. The basis for generating this table is the calculation of motor torque vs stepping frequency and phase angle and of the motion simulation.

An experimental control system was implemented on a small computer, which provided the memory for the logic and the delay-interval table. The motor was loaded with the paper carriage of a high-speed printer under various load conditions. Positioning control and inherent speed control were excellent. The performance was higher than with the conventional closed-loop control mode because of the efficient velocity-time characteristic, which eliminates the low-speed phase.

## **Acknowledgments**

The authors acknowledge the contributions of D. Koegler, H. Weis, and H. Ulland to the design and construction of the control computer. They also performed the measurements.

#### References

- B. C. Kuo, "Step Motors as Control Devices," Proceedings of the First Conference on Incremental Motion Control Systems and Devices, Urbana, IL, 1972, p. 1.
- K. S. Kordik, "The Step Motor-What It Is and Does," Proceedings of the Third Annual Symposium on Incremental Motion Control Systems and Devices, Urbana, IL, 1974, p. A1.
- J. B. Pawletko, "Approaches to Stepping Motor Controls," Electromechanical Design 16, No. 12, 26 (November-December 1972).
- B. C. Kuo, "Control Aspects of Step Motors," Proceedings of the Second Annual Symposium on Incremental Motion Control Systems and Devices, Urbana, IL, 1973, p. 335.
- B. C. Kuo and G. Singh, "Closed Loop and Speed Control of Step Motors," Proceedings of the Third Annual Symposium on Incremental Motion Control Systems and Devices, Urbana, IL. 1974, p. C-1.

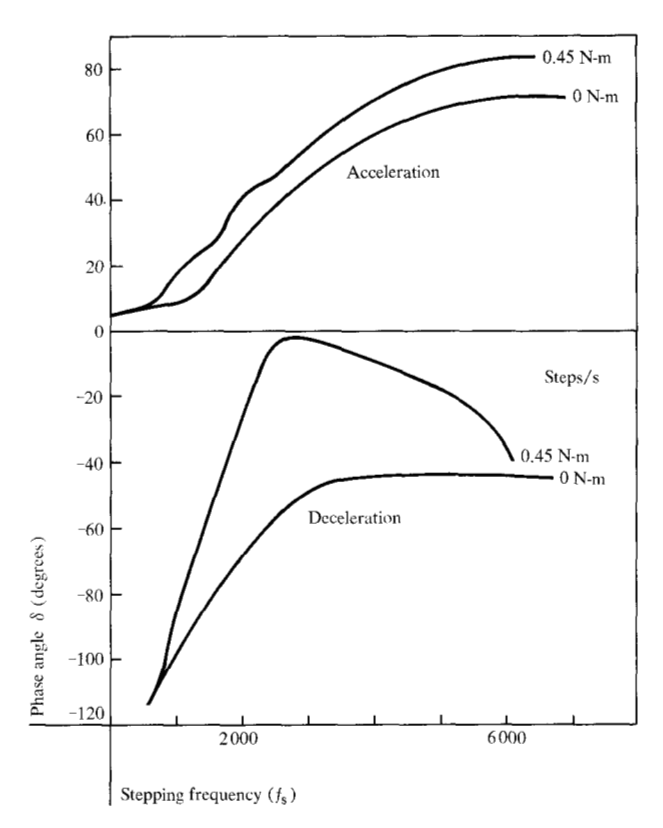


Figure 10 Measurements of phase angle vs stepping frequency, demonstrating the velocity control behavior of the system.

- J. Maginot and W. Oliver, "Step Motor Drive Circuitry and Open Loop Control," Proceedings of the Third Annual Symposium on Incremental Motion Control Systems and Devices, Urbana, IL, 1974, p. B-1.
- J. Tal, "Torque Boundaries for Permanent Magnet Step Motors," Proceedings of the Fourth Annual Symposium on Incremental Motion Control Systems and Devices, Urbana, IL, 1975, p. M-1.

Received May 13, 1975

B. Bechtle, of the Development Laboratory at Boeblingen, is currently on assignment at the IBM Thomas J. Watson Research Center, Yorktown Heights, New York 10598; Messrs. Schünemann, Skudelny, and Zimmerman are with IBM Deutschland GmbH, Development Laboratory, Schoenaicher Strasse 220, 703 Boeblingen, Germany.